Ion-momentum imaging of resonant dissociative-electron-attachment dynamics in methanol

D. S. Slaughter,[1,*] D. J. Haxton,[1] H. Adaniya,[1] T. Weber,[1] T. N. Rescigno,[1] C. W. McCurdy,[1,2] and A. Belkacem[1]

[1]*Lawrence Berkeley National Laboratory, Chemical Sciences, Berkeley, California 94720, USA*

[2]*Departments of Chemistry and Applied Science, University of California, Davis, California 95616, USA*

(Received 6 March 2013; published 28 May 2013)

A combined experimental and theoretical investigation of the dissociative-electron-attachment (DEA) dynamics in methanol are presented for the Feshbach resonance at 6.5-eV incident electron energy. Highly differential laboratory-frame momentum distributions have been measured for each fragmentation channel using a DEA reaction microscope. These measurements are combined with calculations of the molecular-frame electron attachment probability in order to investigate the dynamics of the dissociating methanol transient negative anion. In contrast to previous comparisons between water and methanol [Curtis and Walker, J. Chem. Soc., Faraday Trans. **88**, 2805 (1992); Prabhudesai, Nandi, Kelkar, and Krishnakumar, J. Chem. Phys. **128**, 154309 (2008)], we find subtle differences in the dissociation dynamics of the two fragment channels that are direct evidence of planar symmetry-breaking of warm methanol in its electronic ground state. We also find that the DEA fragmentation does not strictly follow the axial recoil approximation and we describe the dynamics that enable an accurate prediction of the fragment angular distributions.

DOI: 10.1103/PhysRevA.87.052711 PACS number(s): 34.80.Ht

I. INTRODUCTION

Low-energy free electrons are widely considered to play an important role in the radiation-induced chemistry of biomolecules [1] and organic chemistry in the interstellar medium [2]. Dissociative electron attachment (DEA) is one of the primary fundamental interactions that drives free-electron chemistry and attracts considerable interest, not only for the need to understand electron-induced molecular breakup and negative ion production in nature but also to understand them in systems of technological interest [3].

Both gaseous methanol and its ice are ubiquitous in interstellar clouds and comets, but the mechanisms of methanol synthesis in these systems are not well understood, although low-energy electrons are likely to play an important role [4,5]. Free-electron-driven chemistry also provides many reaction pathways leading to more complex molecules of which methanol may be an intermediate [2]. On Earth, methanol has widely been proposed as a potential large-scale alternative to fossil fuels, as it can be produced both agriculturally and synthetically. Today, industrial production of methanol is typically achieved by the reaction of synthesis gas (mixtures of H_2, CO_2, and CO) in the presence of a $Cu/Zn/Al_2O_3$ catalyst at high temperatures and pressures [6]. A similar scheme has been proposed for storage of CO_2 and electrical energy [7] and it is possible that DEA or the time-reverse process, associative detachment, plays an important role in these industrial applications.

Several experimental studies have been conducted on DEA to methanol in the past, including measurements of the translational kinetic energy release (KER) [8,9] and velocity slice imaging [11] of the dissociation products. Kühn *et al.* [9] found evidence of hydrogen scrambling in the production of OH^- in the 10.5-eV resonance in their measurements of DEA relative cross sections and KER spectra in methanol over electron energies spanning 0 to 17 eV. Curtis and Walker [8] extended the study to the H^- ion channel, making comparisons between the three Feshbach resonances in methanol and the Feshbach resonances in the relatively well-understood water molecule [8,10–20], in addition to comparing the DEA spectra to the corresponding parent Rydberg states in both vuv photoabsorption spectra and near-threshold electron-energy-loss spectra. They identified each of the first two Feshbach resonances to be due to the promotion of an electron from either of the highest-lying occupied orbitals, $(7a')^2$ or $(2a'')^2$, of methanol in its ground state, having planar (C_s) symmetry, and simultaneous electron attachment to the 3*s* Rydberg orbital, the 6.5- and 8-eV resonances being $^2A''$ $[(2a'')^1(3s)^2]$ and $^2A'$ $[(7a')^1(3s)^2]$, respectively.

More recently, Ibănescu *et al.* [21] provided further insight into these resonances by comparing their high-precision measurements of DEA ion yields, photoelectron spectra, and vibrational excitation cross sections from several alcohols, characterizing a previously unknown shape resonance at around 3 eV. Ibănescu and Allan [22] followed this with a time-dependent density-functional-theory description of the dynamics of the first two Rydberg states in methanol, predicting that the dynamics of dissociation of the 1 $^2A''$ Feshbach resonance in the methanol anion would follow the dynamics of the parent Rydberg excited state [23] of the molecule.

Prediction and measurement of the dynamics of the methanol anion dissociation processes are formidable challenges from both theoretical and experimental perspectives. In general, detailed measurement and analysis of the dynamics of DEA to polyatomic molecules have, until recently, been limited to small molecules containing only a few atoms. Our understanding of multidimensional dynamics resulting from DEA are hindered by the few elements of symmetry and many degrees of freedom that exist in larger polyatomics. Methanol is one of the simplest systems that possesses relatively weak planar symmetry and many vibrational modes, presenting an accessible case for measuring, modeling, and understanding DEA dynamics. In this paper, we investigate the electron attachment probability in the molecular frame

*DSSlaughter@lbl.gov

and DEA fragmentation momentum images to explore the roles of symmetry-breaking and dissociation dynamics in DEA to polyatomic molecules. We employ multidimensional ion-momentum imaging and *ab initio* theory to describe the DEA process in methanol, focusing on aspects that distinguish this more complex system from the simpler system of water $^2B_1$.

II. EXPERIMENTAL

A full description of the experimental technique has been presented recently [24]; therefore only a brief overview is given here. A low-energy pulsed electron beam, with an energy spread measured to be about 0.8 eV full width at half maximum (FWHM), was produced by a commercially acquired tunable electron gun and guided by a coaxial magnetic field to intersect with the methanol vapor target at an angle of 90°. The target was prepared by driving methanol vapor of typically a few Torr through a stainless steel capillary with an inner diameter of 0.3 mm. All anions formed in the collision region, defined as the intersection of the effusive beam and the electron beam, were extracted by a delayed extraction field pulse that was synchronized with the electron gun pulse into the position- and time-focusing spectrometer. Most scattered electrons were prevented from entering the spectrometer through deflection by the magnetic field and by the extensive spectrometer and detector shielding, which also decoupled the detector from the pulsed extraction electrode. Position and arrival times of the anions were detected by a position- and time-sensitive detector, consisting of a microchannel plate and delay-line anode, and recorded event-by-event. This position and time sensitivity enabled both three-dimensional momentum imaging and mass sensitivity of the singly charged fragment anions. The performance and calibration of the spectrometer were periodically checked against the well-known momentum spectrum of O^- from DEA to O_2 [25].

In order to distinguish between dissociation of the methyl and hydroxyl functional groups, a series of otherwise identical experiments were performed on partially deuterated isotopologs of methanol, including methanol deuterated at the hydroxyl site (CH_3OD) and methanol deuterated at the methyl site (CD_3OH). By separating H^- and D^- in the spectrometer time-of-flight (TOF) spectra, the contributions of each functional group to the DEA process were identified. In addition, the data for the isotopologs were compared to undeuterated methanol in order to determine the significance of any isotope effects on the dissociation dynamics.

III. THEORETICAL

To connect the theoretical results, calculated in the molecular frame, to the observed laboratory-frame angular distributions we calculate the entrance amplitude, formally defined as $V(\theta,\phi;\mathbf{S}) = \langle \Psi_{\rm bg}^+(\theta,\phi;\mathbf{S})|H_{\rm el}|\Psi_{\rm res}(\mathbf{S})\rangle$, where $\Psi_{\rm bg}^+$ is a background scattering function with a plane-wave incident on the target in the direction θ,ϕ; $\Psi_{\rm res}$ is the resonance wave function; $H_{\rm el}$ is the electronic part of the Hamiltonian; and $\mathbf{S}$ labels the internal coordinates of the molecule. The electron attachment probability, a function of θ and ϕ expressed relative to the dissociation axis in the molecular frame, is computed from the squared modulus of the entrance amplitude [19]. In practice, we can evaluate the entrance amplitude in terms of quantities obtained from an analysis of the calculated fixed-nuclei S matrix, as outlined in Ref. [19].

The attachment probability can be directly related to a laboratory-frame angular distribution under the assumption that the fragments recoil at a given angle in the molecular frame. Within a semiclassical treatment of nuclear motion this means that the overall rotation of the molecule is slow compared to dissociation, and the molecular frame recoil axis is constant over the Franck-Condon region of the neutral.

For axial recoil the recoil angle is equal to the initial angle between the recoil fragments' centers of mass, and here we consider deviations in terms of the number of degrees relative to axial. The attachment probability is averaged over the coordinate ϕ azimuthal to the recoil axis to produce the laboratory-frame fragment distribution as a function of θ, the scattering angle of the recoil vector relative to the incident electron. The average over ϕ corresponds to averaging over initial orientations of the molecule, where ϕ is the last Euler angle.

The observed angular distributions are due to attachment at molecular geometries throughout the Franck-Condon region of the neutral. Attachment at the equilibrium geometry of the neutral, in which the molecule is symmetric with respect to reflection and the resonance belongs to the A'' point group, yields an angular distribution that is zero in the forward and backward directions. An average over asymmetric vibrational modes is required to obtain a qualitatively accurate result. The methanol molecule has 12 vibrational modes, 5 antisymmetric and 7 symmetric. At the temperature of the experiment only the torsional mode, the lowest-energy mode, is excited. Fixing the torsional mode, the calculations have been averaged over the remaining 4 asymmetric modes and 1 of the symmetric modes (CH_3 deformation) of the molecule. Two-point hermite quadrature in each mode is employed, using a grid of 32 internuclear geometries, which is found to be sufficient for reasonable convergence. Results are averaged over the torsional mode using the classical partition function at a temperature approximating the experimental target temperature.

Single-channel scattering calculations were performed using the complex Kohn method [26,27]. Dunning's augmented correlation consistent polarized valence triple zeta (aug-cc-pvdz) basis [28,29] was employed. At its equilibrium geometry, methanol is nominally described by the electronic configuration $([1\text{-}6]a')^1 2\ (1a'')^2\ (7a')^2\ (2a'')^2$, while the transient A'' anion state has the configuration $([1\text{-}6]a')^1 2\ (1a'')^2\ (7a')^2\ (2a'')^1\ (8a')^2$. In our calculations, the neutral and anion states were described by multiconfiguration wave functions, with the $[1\text{-}6]a'$ and $1a''$ orbitals restricted to be doubly occupied, and a complete active space consisting of the $2a''$ and $7\text{-}10a'$ orbitals. The orbitals were defined by a state-averaged multiconfiguration self-consistent field calculation using the Columbus quantum chemistry program [30–34].

The orbitals were optimized to minimize a weighted average of energies of six neutral and five discretized anion states. The variational trial function for the scattering calculations included the electronically elastic channel functions (neutral ground-state times scattering orbitals outside the active space) plus all additional $(N+1)$-electron terms that could be constructed from the active space orbitals.

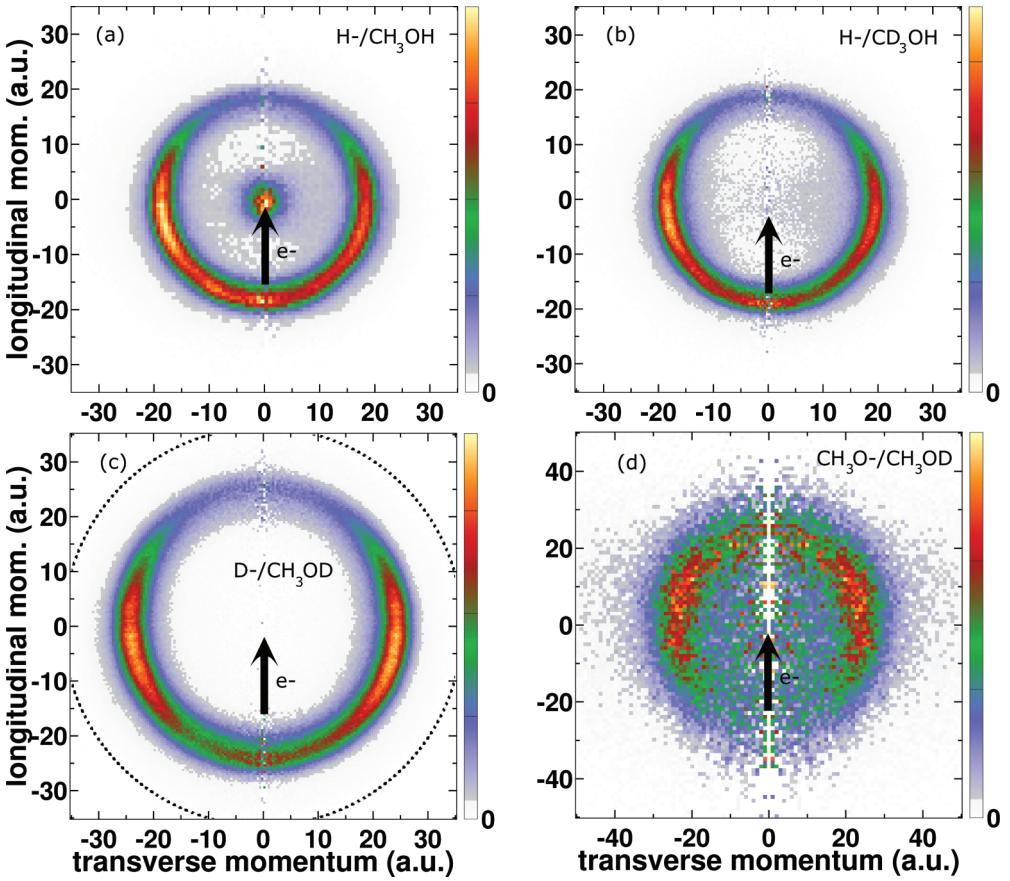

FIG. 1. (Color online) Measured momentum distributions of ions resulting from DEA to methanol at 6.3 eV nominal electron beam energy. The electron beam direction is indicated by an arrow and the color map is the unnormalized ion yield on a linear scale. (a) H^-/CH_3OH; (b) H^-/CD_3OH; (c) D^-/CH_3OD, the dashed curve indicates the D^- momentum in the absence of any isotope effect; (d) CH_3O^-/CH_3OD.

Angular momentum channels up to $l = 5$ were included in the scattering calculation. Since only the electronically elastic channel is explicitly included, the calculation produces pseudoresonances at energies above the electronically inelastic thresholds; however, the physical state is clearly identified through its dominant configuration.

IV. RESULTS

The measured three-dimensional momentum spectrum of H^- resulting from DEA to methanol is displayed in Fig. 1(a). The transverse momentum is an average over the coordinates transverse to the electron beam direction (the latter being upwards, as indicated by an arrow), and the left and right sides of the image correspond to ion momenta away from and towards the detector, respectively. The distribution exhibits a wide peak in the backward direction, with respect to the incident electron and the absolute momentum is found to be sharply peaked at 18 atomic units (a.u.). In Fig. 1(b) we present the H^- spectrum at the same incident electron energy for the partially deuterated target, CD_3OH. The absence of the low-energy H^- peak at the momentum origin that was observed in undeuterated methanol clearly indicates that it is attributed entirely to a C-H break within the methyl functional group. This was further corroborated by the disappearance of the equivalent peak in the D^- spectra of the complementary experiments on CH_3OD [Fig. 1(c)] and the observation of only very-low-energetic H^- from CH_3OD and D^- from CD_3OH (not shown) for the same electron energy. The D^-/CH_3OD spectrum of Fig. 1(c) differs in the absolute magnitude of the ring created by dissociation of the heavier D^- and the slightly lower relative ion yield in the backwards longitudinal direction. From simple conservation of energy and momentum arguments, we expect the momentum of D^- following DEA to CH_3OD to be about a factor of 1.98 larger than that of H^- from CD_3OH or normal methanol. As illustrated in Figs. 1(a)–1(c), this is not the case and the D^- momentum is suppressed to about 25 a.u. from the expected 36 a.u.

As the electron beam energy is increased from the low-energy side to the high-energy side of the resonance the absolute momentum and corresponding kinetic energy of D^- increases and broadens with increasing electron energy, as shown in the D^- kinetic energy spectra of Fig. 2. This indicates that the available energy following DEA is always partitioned between the translational KER of both fragments and the rovibrational energy in the neutral methoxy radical.

In addition to the primary DEA fragmentation channel due to an O-D bond break leading to a deuterium anion and a methoxy radical, in Fig. 1(d) we also present the momentum spectrum of the complementary channel producing atomic deuterium and the methoxide anion CH_3O^-. The total ion

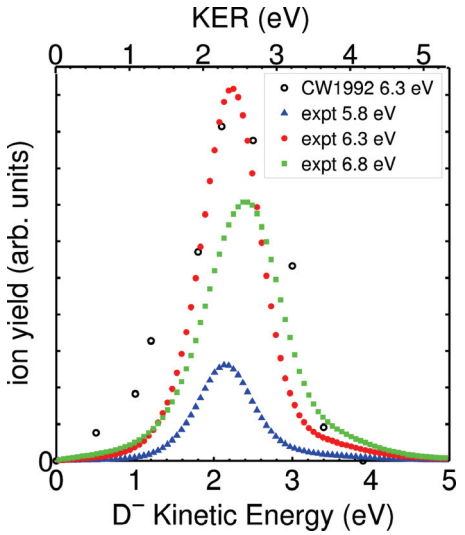

FIG. 2. (Color online) Measured kinetic energy of D^- (solid symbols) and corresponding KER of the two-body dissociation, resulting from DEA to CH_3OD at electron beam energies specified in the plot. Where not shown, the error bars, representing one standard deviation of the statistical uncertainty, are smaller than the symbols in each plot. The data of Curtis and Walker [8] (empty circles) are also displayed for comparison. The total ion yield is normalized to the relative cross section of Ibănescu *et al.* [21].

yield of CH_3O^- in the present experiments was one to a few percent compared to the more favorable channel leading to D^-. While we did observe a comparable yield of CH_3O^- in the experiments on undeuterated methanol, the ion spectra contained an appreciable background of CH_2O^- that prevented a complete momentum analysis. The momentum spectrum of CH_3O^- following DEA to CH_3OD at 6.5-eV electron energy is displayed in Fig. 1(d). Since both energy and momentum are conserved, the total KER of both fragments is determined as 16.5 and 1.06 times the measured anion kinetic energy in the CH_3O^- and D^- channels, respectively. Comparing the CH_3O^-/CH_3OD kinetic energy distribution of Fig. 3 to

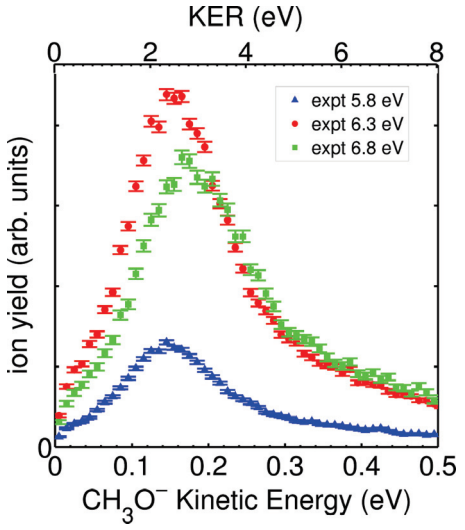

FIG. 3. (Color online) Same as Fig. 2, but for the methoxide anion CH_3O^- following DEA to CH_3OD.

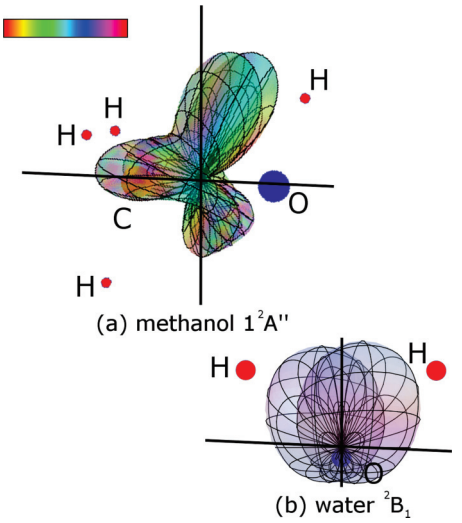

FIG. 4. (Color online) Quantum mechanical entrance amplitude as a function of the incident electron angle in the molecular frame (a) for electron attachment to the $1\,^2A''$ Feshbach resonance of methanol in its equilibrium geometry. The positions of the nuclei are represented by dots and the magnitude and the phase of the entrance amplitude are indicated by the radial distance and the inset color scale, respectively. (b) The entrance amplitude for the $^2B_1$ resonance in water (from Ref. [14]). In each case, a node in the entrance amplitude is present in the molecular plane, as dictated by the symmetry of the resonance.

that of the complementary channel D^-/CH_3OD (Fig. 2), we see a broader KER distribution in the CH_3O^- channel and a peak KER comparable to that of the D^- channel. The thermodynamic thresholds for the $D + CH_3O^-$ and $H^- + CD_3O$ limits are 2.97 and 3.75 eV, respectively [8]. The small KER in the CH_3O^- channel implies an increased transfer of kinetic energy into vibrational excitation of the molecular fragment, manifesting as a broadening of the ion kinetic energy distribution.

The variation of the calculated entrance amplitude with angle of incidence in the molecular frame, for electron attachment to the $1\,^2A''$ Feshbach resonance in methanol at its equilibrium geometry, is illustrated in Fig. 4(a). Due to the A'' symmetry of the resonance, the data feature a sharp minimum in the C-O-H plane that we expect becomes shallow, or even completely filled, when the symmetry is broken by excitation of the torsional mode at the finite target temperature of the experiment. Upon comparison with the entrance amplitude of the water $^2B_1$ resonance [14] displayed in Fig. 4(b), the contrast is striking. The substitution of the hydrogen atom with a methyl group has a surprisingly large impact on the probability for electron attachment as a function of the incident electron angle.

V. DISCUSSION

In this investigation we have identified three dissociation channels resulting from DEA to methanol in the 6.5-eV electron energy region. One channel, leading to H^- (or D−) from the (deuterated) methyl functional group, results in very little H^- kinetic energy, which is consistent with the three-body dissociation $H^- + H + CH_2O$. This channel was also found

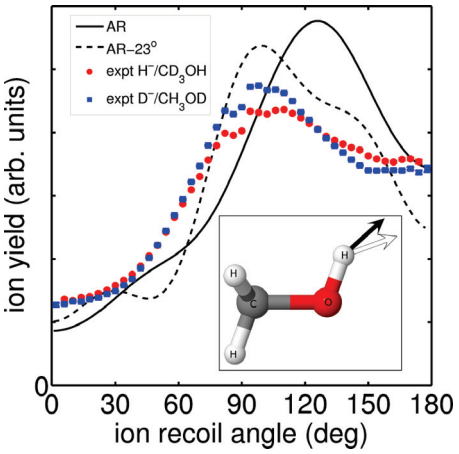

FIG. 5. (Color online) Measured angular dependence of H^- from DEA to CD_3OH (circles) and of D^- from DEA to CH_3OD (squares) at a nominal electron beam energy of 6 eV. Where not shown, the error bars, representing one standard deviation of the statistical uncertainty, are smaller than the symbols in each plot. Also shown are the unmodified axial recoil prediction as calculated by averaging over asymmetric modes (solid curve) and the prediction for recoil 23° off-axis (dash curve), parallel to the gradient illustrated in the inset schematic. The experimental data are normalized to the theory. Inset: Gradient of the $^2A''$ potential energy surface with respect to the motion of the hydroxyl hydrogen atom in the molecular frame, with CH_3O fixed, illustrated by the direction of the white arrow. The gradient vector is 23° from the axis connecting the center of mass with the hydrogen atom (black arrow) and is used as the recoil axis to calculate the off-axis result.

to be present at the two higher-resonant electron energies of 8.0 and 10.5 eV; therefore it is possible that it does not originate from the 6.5-eV Feshbach resonance and could be due to a broad resonance at a nearby energy such as that found in DEA to ethanol [21]. The two dissociation channels that most clearly originate from the 6.5-eV Feshbach resonance are D^- + CH_3O and D + CH_3O^-.

The measured angular distributions of D^- and CH_3O^- (Figs. 5 and 6, respectively) both exhibit a similar structure, with the former having a peak at about 105° with respect

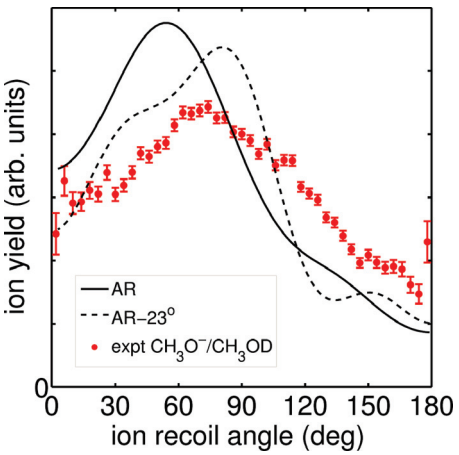

FIG. 6. (Color online) Same as Fig. 5, but for CH_3O^- resulting from DEA to CH_3OD.

to the forward incident electron direction (0°) and the latter having a peak at the same angle from the backward electron direction (180°). While it has been widely assumed that electron attachment launches a nuclear wave packet to the $1\,^2A''$ intermediate state, dissociation on that potential energy surface (PES) provides only one of the two possible final electronic states. The second final electronic state is the result of a nonadiabatic transition from that surface onto an intersecting surface. The observation that the two fragments, D^- and CH_3O^-, each originating from a different dissociation channel, recoil in opposite directions suggests that both the intermediate PES and the PES leading to the second final state are likely to be strongly repulsive along the O-H stretch coordinate.

Ibănescu *et al.* [21] measured a peak in the CH_3O^- channel of their DEA spectra near the thermodynamic threshold of 2.97 eV. They attributed the narrow feature to a broad σ^* shape resonance that exists at very low electron impact energies in vibrational excitation, but is truncated in DEA on both the low-energy side of the resonance, by the relatively high thermodynamic threshold for the reaction, and on the high-energy side, by the decreasing lifetime of the resonance with respect to autodetachment. The present KER measurements are of the same final electronic state: the methoxide anion and a deuterium radical, each in their electronic ground states. The measurements exhibit an increase in the KER from 2.4 to 3.0 eV over the incident electron energy range of 5.8 to 6.8 eV. This implies a final methoxide rovibrational energy of 0.4 to 0.8 eV at the limit of dissociation. We compare this with the $D^- + CH_3O$ channel, measured in the same experiment, where the equivalent analysis yields a dissociation limit between 0.0 and 0.5 eV above the thermodynamic threshold of 3.75 eV.

We have confirmed that the $CH_3O^- + D$ dissociation limit has an ion yield much smaller than that of $D^- + CH_3O$. This ion yield measurement may be influenced by the finite autodetachment lifetime of the methoxide anion, which depends on its vibrational energy and may be comparable to its TOF of ∼7.8 μs before reaching the detector. We note that the electron affinity of the methoxy radical is 1.57 eV [35], which is substantially larger than the measured vibrational energy of 0.4–0.8 eV, so we do not expect the lifetime to be significantly reduced. If we consider the methoxide anion to be relatively long-lived in this case, then it is a minor channel that is the result of a nonadiabatic transition from the $1\,^2A''$ state to a second state. The geometry of the methoxide anion is expected to differ only marginally from that of the methoxy radical [36,37]; therefore it is possible that the two PES approach each other at large O-H separation if enough rovibrational energy is present in the anion, which is well supported by the KER spectrum of Fig. 3. The second PES is possibly that of the σ^* shape resonance discovered by Ibănescu *et al.* [21].

Curtis and Walker [8] and Prabhudesai *et al.* [11] demonstrated that the kinetic energy and angular distributions of H^- from DEA to methanol at this resonance energy are remarkably similar to those of the $^2B_1$ Feshbach resonance in H_2O at electron impact energies around 6 eV [14,17,38]. Curtis and Walker [8] argued this from the comparison of the dependence of the DEA cross section on the electron energy and the measured ion kinetic energy, while Prabhudesai *et al.* [11] measured similarities in their measured velocity slice

images from water, methanol, and acetic acid. While we do find similarities in the H^- dissociation from the hydroxyl site of methanol and water for these two Feshbach resonances, differences clearly arise between the two ion yields at forward and backward angles with respect to the electron beam. This is primarily due to the perfect planar symmetry of water and the node in the entrance amplitude in the molecular plane [17]. In contrast, H^- dissociation from methanol contributes some 30% and 70% of the maximum yield in the forwards and backwards directions, respectively, as illustrated in Fig. 5. This is a direct consequence of vibrational motion breaking the reflection symmetry of the molecule, as previously discussed.

The measured angular distributions of H^- (D^-) ion channels following an O-H (O-D) break in the transient negative ion are displayed alongside the prediction based upon the axial recoil approximation in Fig. 5. In the impulse approximation the recoil axis corresponds with the gradient of the PES at the initial geometry of the neutral. This angle is calculated as 23° from axial, as illustrated in the inset of Fig. 5. Taking the heavy CH_3O fragment to be fixed, 23° off-axis is then also the angle of recoil in the molecular frame. As shown in Fig. 5, the angular distribution calculations using this recoil angle yield a much better comparison with the experimental data than does the axial recoil result. The comparison between theory and experiment gives strong evidence that the dissociation indeed proceeds via an opening of the C-O-H bond angle, consistent with recoil along the gradient of the potential energy surface at the initial geometry.

The angular distribution of the methoxide anion following DEA to CH_3OD is displayed in Fig. 6. While the experimental data are a direct measurement taken in the same experimental run as the D^- distribution, the theoretical results are simply reflected about 90° compared to the H^- distributions of Fig. 5. In both fragmentation channels, the agreement between the experimental data and the 23° of-axis result is outstanding, with the only discrepancies being the broadened features that we observe in the experimental data. These features are not due to the limited angular resolution of the experiment, which we estimate to be typically better than 5° FWHM and 20° FWHM for H^- and CH_3O^-, respectively, but are likely due to the effect of the sampling of vibrational modes not considered in the calculations and possibly due to dissociation dynamics involving breakdown of a constant recoil angle approximation on the $1\,^2A''$ PES.

VI. CONCLUSIONS

We have investigated the dynamics of DEA to methanol for the low-energy Feshbach resonance at 6.5 eV, using a combination of ion-momentum imaging and *ab initio* theory. We have calculated the angular distribution of fragments from the two observed dissociation channels following an O-H break and find very good agreement with the measured ion-momentum distributions. The angular distributions of the recoiling fragments were found to deviate significantly from the axial recoil approximation that was used previously to accurately describe the dynamics in the analogous $^2B_1$ resonance in water, [14,17,19] primarily due to opening of the C-O-H bond angle in the transient methanol anion.

The present measurements highlight the breakdown in symmetry that occurs in the methanol molecule at room temperature that has a strong influence on the electron attachment probability in the molecular frame. In a further departure from the dynamics of the $^2B_1$ resonance in water, which leads to only one final state [20], DEA to methanol at 6.5 eV produces two final states following two-body dissociation and we find evidence that both states are connected to the Feshbach resonance by a conical intersection. This work demonstrates that ion-momentum imaging and *ab initio* theory can be employed to describe DEA dynamics in polyatomic molecules and is a crucial step in the development of the DEA ion imaging technique to study dynamics in more complex systems.

ACKNOWLEDGMENT

This work was supported by the Director, Office of Science, Office of Basic Energy Sciences, and by the Division of Chemical Sciences, Geosciences, and Biosciences of the US Department of Energy at LBNL under Contract No. DE-AC02-05CH11231.

[1] I. Baccarelli, I. Bald, F. A. Gianturco, E. Illenberger, and J. Kopyra, Phys. Rep. **508**, 1 (2011).
[2] T. Millar, E. Roueff, S. Charnley, and S. Rodgers, Int. J. Mass Spectrom. Ion Processes **149-150**, 389 (1995).
[3] I. Utke, P. Hoffmann, and J. Melngailis, J. Vac. Sci. Technol. B **26**, 1197 (2008).
[4] C. J. Bennett, S. Chen, B. Sun, A. H. H. Chang, and R. I. Kaiser, Astrophys. J. **660**, 1588 (2007).
[5] A. Wada, N. Mochizuki, and K. Hiraoka, Astrophys. J. **644**, 300 (2006).
[6] M. Behrens, F. Studt, I. Kasatkin, S. Kuhl, M. Havecker, F. Abild-Pedersen, S. Zander, F. Girgsdies, P. Kurr, B.-L. Kniep, M. Tovar, R. W. Fischer, J. K. Norskov, and R. Schlogl, Science **336**, 893 (2012).
[7] G. A. Olah, Angew. Chem., Int. Ed. **44**, 2636 (2005).
[8] M. G. Curtis and I. C. Walker, J. Chem. Soc., Faraday Trans. **88**, 2805 (1992).
[9] A. Kühn, H.-P. Fenzlaff, and E. Illenberger, J. Chem. Phys. **88**, 7453 (1988).
[10] V. S. Prabhudesai, D. Nandi, A. H. Kelkar, and E. Krishnakumar, J. Chem. Phys. **128**, 154309 (2008).
[11] V. S. Prabhudesai, N. B. Ram, G. Aravind, P. Rawat, and E. Krishnakumar, J. Phys.: Conf. Ser. **80**, 012016 (2007).
[12] M. Jungen, J. Vogt, and V. Staemmler, Chem. Phys. **37**, 49 (1979).
[13] J. Fedor, P. Cicman, B. Coupier, S. Feil, M. Winkler, K. Guch, J. Husarik, D. Jaksch, B. Farizon, N. J. Mason, P. Scheier, and T. D. Märk, J. Phys. B **39**, 3935 (2006).

[14] H. Adaniya, B. Rudek, T. Osipov, D. J. Haxton, T. Weber, T. N. Rescigno, C. W. McCurdy, and A. Belkacem, Phys. Rev. Lett. **103**, 233201 (2009).
[15] P. Rawat, V. S. Prabhudesai, G. Aravind, M. A. Rahman, and E. Krishnakumar, J. Phys. B **40**, 4625 (2007).
[16] N. B. Ram, V. S. Prabhudesai, and E. Krishnakumar, J. Phys. B **42**, 225203 (2009).
[17] H. Adaniya, B. Rudek, T. Osipov, and A. Belkacem, J. Phys.: Conf. Ser. **194**, 012031 (2009).
[18] D. J. Haxton, Z. Zhang, H.-D. Meyer, T. N. Rescigno, and C. W. McCurdy, Phys. Rev. A **69**, 062714 (2004).
[19] D. J. Haxton, C. W. McCurdy, and T. N. Rescigno, Phys. Rev. A **73**, 062724 (2006).
[20] D. J. Haxton, T. N. Rescigno, and C. W. McCurdy, Phys. Rev. A **75**, 012711 (2007).
[21] B. C. Ibănescu, O. May, A. Monney, and M. Allan, Phys. Chem. Chem. Phys. **9**, 3163 (2007).
[22] B. C. Ibănescu and M. Allan, Phys. Chem. Chem. Phys. **10**, 5232 (2008).
[23] Y. Wen, J. Segall, M. Dulligan, and C. Wittig, J. Chem. Phys. **101**, 5665 (1994).
[24] H. Adaniya, D. S. Slaughter, T. Osipov, T. Weber, and A. Belkacem, Rev. Sci. Instrum. **83**, 023106 (2012).
[25] P. Chantry and G. Schulz, Phys. Rev. **156**, 134 (1967).
[26] T. N. Rescigno, C. W. McCurdy, A. E. Orel, and B. H. L. III, in *Computational Methods for Electron-Molecule Collisions*, edited by W. M. Huo and F. A. Gianturco (Plenum, New York, 1995).
[27] T. N. Rescigno, B. H. Lengsfield III, and C. W. McCurdy, in *Modern Electronic Structure Theory*, Part 1, edited by D. R. Yarkony (World Scientific, Singapore, 1995), pp. 501–588.
[28] T. H. Dunning, J. Chem. Phys. **90**, 1007 (1989).
[29] R. A. Kendall, T. H. Dunning, and R. J. Harrison, J. Chem. Phys. **96**, 6796 (1992).
[30] H. Lischka, R. Shepard, F. B. Brown, and I. Shavitt, Int. J. Quantum Chem., Quantum Chem. Symp. **15**, 91 (1981).
[31] R. Shepard, I. Shavitt, R. M. Pitzer, D. C. Comeau, M. Pepper, H. Lischka, P. G. Szalay, R. Ahlrichs, F. B. Brown, and J. Zhao, Int. J. Quantum Chem., Quantum Chem. Symp. **22**, 149 (1988).
[32] H. Lischka, R. Shepard, R. M. Pitzer, I. Shavitt, M. Dallos, T. Müller, P. G. Szalay, M. Seth, G. S. Kedziora, S. Yabushita, and Z. Zhang, Phys. Chem. Chem. Phys. **3**, 664 (2001).
[33] H. Lischka, T. Müller, P. G. Szalay, I. Shavitt, R. M. Pitzer, and R. Shepard, WIREs **1**, 191 (2011).
[34] H. Lischka, COLUMBUS, an ab initio electronic structure program, Release 7.0 (2012).
[35] P. C. Engelking, G. B. Ellison, and W. C. Lineberger, J. Chem. Phys. **69**, 1826 (1978).
[36] D. A. Weil and D. A. Dixon, J. Am. Chem. Soc. **107**, 6859 (1985).
[37] K. B. Wiberg, G. B. Ellison, J. M. McBride, and G. A. Petersson, J. Phys. Chem. A **117**, 213 (2013).
[38] D. S. Belic, M. Landau, and R. I. Hall, J. Phys. B **14**, 175 (1981).